CHALMERS
UNIVERSITY OF TECHNOLOGY

Optimization of sound absorber

Design of sound absorber for the study of sound incidence in long narrow spaces such as corridors

Master's thesis in Master Program Sound and Vibration

RUSHI GANAPATHI APADANDA

DEPARTMENT OF ARCHITECTURE AND CIVIL ENGINEERING

CHALMERS UNIVERSITY OF TECHNOLOGY
Gothenburg, Sweden 2024
www.chalmers.se

Master's thesis ACEX30

Optimization of sound absorber

Design of sound absorber for the study of sound incidence in long narrow spaces such corridors

Rushi Ganapathi Apadanda

CHALMERS
UNIVERSITY OF TECHNOLOGY

Department of Architecture and Civil Engineering
Division of Building Technology
Building Physics Group
Chalmers University of Technology
Gothenburg, Sweden 2024

Optimization of sound absorber
Design of sound absorber for the study of sound incidence in public spaces such as corridors

Rushi Ganapathi Apadanda

Supervisor: Professor Krister Larsson, Applied Acoustics, Chalmers
Examiner: Professor Wolfgang Kropp, Applied Acoustics, Chalmers

Department of Architecture and Civil Engineering
Division of Building Technology
Building Physics Group
Chalmers University of Technology
SE-412 96 Gothenburg
Telephone +46 31 772 1000

Cover: Fabricated sound absorber under study.

Department of Architecture and Civil Engineering
Gothenburg, Sweden 2024

Optimization of sound absorber
Design of sound absorber for the study of sound incidence in public spaces such as corridor
Rushi Ganapathi Apadanda
Department of Architecture and Civil Engineering
Chalmers University of Technology

Abstract

Noise mitigation is of importance in areas where health and well-being of individuals is needed and this is especially true in spaces such as schools were noise can hinder learning and cognitive development of children. While acoustical treatment is often focused on classrooms where children and teachers spend large amount of time, corridors remain neglected despite their role in amplifying noise. Corridors with their unique dimension, non-diffuse sound field and source for housing furniture pose a challenge in sound proofing and hence an approach to optimise absorbers is needed and to understand the impact of sound incident angle.

This thesis explores the design and optimization of a sound absorber system tailored for such environments, with a focus on mitigating noise levels in school corridors. The study investigates the performance of a resonant sound absorber, combining a micro-perforated panel, air gap, and porous material, aimed at absorbing sound in the mid-to-high frequency range 850 Hz-4000 Hz in diffuse and non-diffuse sound field conditions.

Using theoretical modeling via the Transfer Matrix Method (TMM) and empirical validation through free-field and diffuse-field measurements, the absorber's performance was analyzed under various sound incidence angles. The results demonstrate that the designed system effectively absorbs sound, with a resonance peak at 2000 Hz. The study also evaluates the impact of parameters such as porous material thickness, perforation size, and air gap on the absorption coefficient for varied incident angle. While the absorber achieved good efficiency, especially at the targeted resonance frequency, edge effects were observed in finite-size samples, leading to overestimation of absorption coefficients in certain cases.

This research highlights the importance of optimizing sound absorbers for non-diffuse sound field environments like corridors, particularly at high frequency range, and offers a practical solution for enhancing acoustic comfort in schools.

Keywords: sound absorber, school corridors, noise mitigation, micro-perforated panel, Transfer Matrix Method, acoustic treatment.

Acknowledgements

With the completion of this master thesis marks my two years journey at the Division of Applied Acoustics and my time at the Chalmers University of Technology. This journey was enriched by the vast knowledge in the field of applied acoustics, fruitful interaction with new friends and acquaintances and the culminative application in this master thesis.

The onset of this master thesis was in collaboration with my supervisor at Efterklang, Krister Larsson. My heartfelt gratitude to Krister for encouraging me to conceive my own ideas, learn from my mistakes and providing valuable feedback when I was stuck in a funk. To my examiner, Wolfgang Kropp, for taking the time to provide valuable insight and guidance to finish my thesis. To Pelle Evensen from the department of FUSE, without whom the fabrication of the absorber would not have been possible. I was fortunate to interact and learn various fabrication methods and techniques from you. Lastly, my classmates at the department who were a great source of strength and with whom countless ideas were discussed and discarded. Thank you.

Rushi Ganapathi Apadanda, Gothenburg, September 2024

Contents

List of Figures **xi**

1 Introduction **1**
1.1 Background . . . 1
1.2 Aim . . . 2
1.3 Limitations . . . 2

2 Theory **3**
2.1 Understanding Corridors . . . 3
2.2 Sound Absorbers . . . 4
2.2.1 Characteristics of Porous Absorber . . . 5
2.2.2 Characteristics of Resonator panel absorbers . . . 6
2.3 Reflection factor,Absorption coefficient and wall impedance . . . 7
2.4 Transfer Matrix Method . . . 10
2.5 Prediction of Sound absorption Coefficient . . . 12

3 Methods **17**
3.1 Determining the absorber system . . . 17
3.2 Theoretical modelling . . . 18
3.2.1 Parameter Analysis . . . 19
3.2.1.0.1 Key take aways . . . 24
3.3 Experimental Validation . . . 25
3.3.1 Measurement method 1 . . . 25
3.3.2 Measurement method 2 . . . 26
3.4 List of equipment . . . 27
3.4.1 Measurement method 1 . . . 27
3.4.2 Measurement method 2 . . . 27

4 Results and Discussion **29**
4.1 Theoretical validation . . . 29
4.1.1 Infinite size Absorber . . . 31
4.1.2 Finite size absorber . . . 32
4.2 Experimental validation . . . 33
4.2.1 Measurement method 1 . . . 33
4.2.2 Measurement method 2 . . . 34

5 Conclusion **37**

List of Figures

1 Basic Types of acoustic absorbers 5
2 Construction of a micro perforated panel 6
3 Sound incidence at an angle ϕ on a locally reacting boundary of impedance Z_g 8
4 Shift in reference plane x 9
5 Acoustic material characterised by transfer matrix $\mathbf{T}$ with wave propagation modelled inside the material 10
6 Acoustic structure composed of several layers of effective parameters,((After, Noé Jiménez, Jean-Philippe Groby, and Vicent Romero-Garcíaet, *The Transfer Matrix Method in Acoustics*,p107,2021)) . . . 11
7 Measurement setup as described in *SS-ISO 13472:1* 13
8 Signal separation procedure as described in *SS-ISO 13472-1* 15

1 Suggested reference for the considered furniture design, from SONESSON INREDNINGAR,After,*https://www.sonesson.se/sortiment/skolskaap-elevskaap/skolskap-elevskap-h3z2.html*) 17
2 Absorption coefficient for changes in Porous absorber material thickness 19
3 Absorption coefficient for changes in flow resistivity 20
4 Absorption coefficient for changes in Air-gap width 21
5 Absorption coefficient for changes hole diameter 22
6 Absorption coefficient for changes in distance between holes 23
7 Measurement setup in the reverberation chamber. 25
8 Free field setup for measurement method 2 26

1 Chosen porous absorber from ISOLINA 30
2 Fabricated sound absorber 30
3 Absorption coefficient obtained by theoretical modelling of the absorber system for (a) Statistical vs normal incidence,(b) variation of angles and (c) certain frequencies over incident angles 31
4 α_{stat} based on theoretical validation of a finite size absorber 32
5 Absorption coefficient of finite size absorber seen with,a)incident angles b)individual frequencies of interest. 33
6 α_{stat} measured over 1/3 octave bands as per ISO 354 in a diffuse field for the fabricated sound absorber system and compared with theoretical calculation 34

7 Absorption coefficient of fabricated absorber,a)$\phi = 0°$,b)$\phi = 30°$,c)$\phi = 45°$,d)$\phi = 0°$,(-)Temporal subtraction method,(-o) Finite absorber, (-x) Infinite absorber 34

1
Introduction

As adults we have walked through many a corridors and in crowded ones too, where we could hardly hear each other. Its loud and annoying at times. Fortunately, we make a rational decision to move away from such spaces. However, walking away poses a challenge if you are a child in preschools since its overstimulating and stressful or a teenager in middle-school for that matter. Hence, its vital for us to address such environments to better manage their health and stimulate learning instead.

This study consists of fabricating a resonant sound absorber whose design and optimization is based on the physical properties of the furniture to be used in school corridors and investigate the impact of said sound field on the performance of the absorber via free field measurements.
This master thesis has been made in collaboration with Efterklang who have been working towards creating functional sound absorbers for public spaces such as schools, offices etc.

1.1 Background

Creating an optimal environment in schools for learning and well being of students and teachers has become a necessity and of utmost importance with the latest survey study mentioned in [11], indicating a steady increase of noise levels in schools through out the EU. Further studies in [16] highlight how noise is perceived differently by children and teachers in preschools, where students are subjected to more noise levels and higher frequency ranges as compared to adults, resulting in an impact in the development of the children. From these studies, it has been made clear that a quite environment is needed to aid learning, improve mental health and prevent long term hearing damage for the teachers and children while clearing indicating the immediate need to address this issue at the early development stage of children.

As such, acoustics and the means of mitigating noise have become integral in early designing and planning of such spaces. There are several ways one can resolve this, good sound insulation from the outdoor environment, erecting noise barriers and using sound absorbers. However, with established preschools, the challenge lies in introducing acoustic treatment which is easy to integrate and multi-functional. Additionally, with much of the acoustic treatment focused in classroom, spaces such as corridors which have significant impact in noise levels and acoustical qualities in

adjoining spaces as studied by Hengling Song [20] are moved away from the spotlight.

In general, the factors contributing to noise source in corridors are footsteps, noise from adjoining rooms and gathering of students during breaks which tend to be amplified due to longer reverberation. As per Swedish regulations, corridors are to be treated as temporary passage ways and hence the resulting noise regulation as seen in the sound level difference $D_{n,T,w}$[dB] between the classroom and corridor stated in [19], is not enough since the source of the noise is considered from classroom. A straight forward solution to reduce noise in corridors is not easy either since they can serve additional purposes such as sources for utilizing furniture for storage and due to their dimensional properties, they tend to deviate from the norm of having a diffuse field condition. By making use of these furniture to house sound absorbers, aids in mitigating noise, diffusing the sound and saving additional cost of absorbers.

1.2 Aim

This thesis has the following aims

- What absorber type is best suited and optimized to have good sound absorption in corridors.
- To investigate the behaviour of sound incident angle on said absorber for non-diffuse field conditions.

1.3 Limitations

The report will focus on the development of the absorber for mid to high frequency region, i.e 800 Hz to 4000 Hz due to the constraints in developing products for the low frequency region, which are dimensional. The use of micro-perforated panel further introduced challenges in fabrication of sub millimeter hole size due to the un-availability of the right machinery. Lastly, the finite size of the absorber led to limitations in faithfully recreating the measurement procedures needed.

2

Theory

The theory chapter is based on a literature study that aims to shed light on the theoretical concepts that drive the goals of this thesis.

2.1 Understanding Corridors

The most notable feature of a corridor is that one of its dimensions are longer than the other two, usually along the length and they are a means of connecting rooms. This makes for an interesting case of a sound field. Due to the presence of hard walled surfaces/boundaries, the concepts of a statistical acoustics which rely on an assumption of diffuse sound field is not applicable since the sound energy reduces with distance [9]. Diffuse sound field in spaces as defined in [23] states that probability of energy transport is the same in all directions and the energy angle of incidence on the room boundaries is random and the frequency above which this is possible is called Schroeder cut-off frequency f_s, given by

$$f_s = 2000 \cdot \sqrt{\frac{T}{V}} \tag{2.1}$$

where V and T are the volume m^3 and reverberation time s, respectively.
The theory from [24] predicts the rate of sound attenuation(Δ in dB/m) outside of the direct field of the source to be:

$$\Delta = 1.7 \cdot \frac{P}{S} \cdot \alpha \tag{2.2}$$

where: P= perimeter of the corridor, S= cross sectional area and α= absorption coefficient of the boundaries.
The above equation provides an insight into the parameters influencing the acoustical design of corridors and frequency range. Longer corridors tend to support the presence of lower frequencies due to the presence of room modes while shorter and narrower corridors emphasize higher frequencies. Additionally, hard walls reflect sound better, particularly at mid-high frequency range.

2.2 Sound Absorbers

The functioning of absorbing materials is linked to the behaviour of sound waves at the interface between two media. When a sound wave hits such a boundary it will normally be diffracted; a part of the energy will be deflected in a direction different from that of the incidence wave. If the boundary surface is large compared with the wavelength one characterizes the process as reflection and the changes in amplitude and phase that take place can be represented by the complex reflection factor (R_p) as

$$R_p = \frac{p_r}{p_i} = |R_p| \cdot e^{j\delta} \tag{2.3}$$

where p_r and p_i are complex pressure amplitudes of the reflected and incident wave and the term $e^{j\delta}$ indicates the phase term.

The part of the energy not deflected and converted to heat or dissipated is governed by the absorption factor or sound absorption coefficient, which is defined for a surface as the ratio of the absorbed energy to the incident energy [23].

$$\alpha = 1 - \frac{E_r}{E_i} \tag{2.4}$$

where E_r and E_i are the reflected acoustic power and incident acoustic power respectively.

Commonly used sound absorbers are:

- **Porous absorbers:** The attenuation of incident sound energy on surface made up of porous material is dissipated by frictional and viscous losses within the pores and by vibration of small fibres of the material. The absorption is large at high frequencies and small at low frequencies.

- **Panel and membrane type:** The attenuation of incident sound energy on an impermeable surface is dissipated by the internal losses of the vibrating system.

- **Resonator absorbers:** The attenuation of incident sound energy on a resonator surface consisting of a cavity with an opening which excites large amplitude of vibrations in the resonant frequency range, dissipates sound energy by means of viscous losses [14].

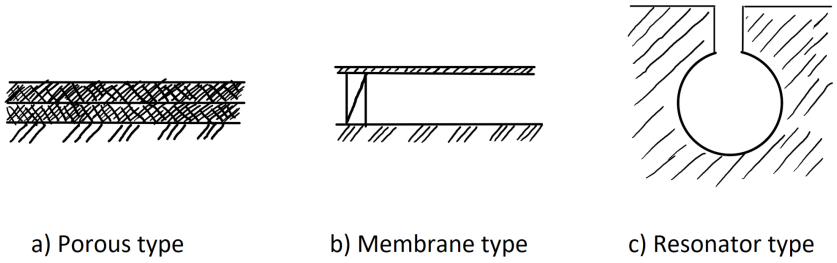

Figure 1: Basic Types of acoustic absorbers

2.2.1 Characteristics of Porous Absorber

There are certain parameters which define the behaviour and performance of a porous absorber. They are as follows:

- **Material thickness** The viscous loss is proportional to the dynamic pressure of the moving air, porous materials can provide more absorption when they are located in positions where the particle velocity of the sound wave is large and this usually the case at distances of $\lambda/4$,$3\lambda/4$...from the wall/boundary. For cases when the absorber is placed against the, its most effective when the thickness of the material is equivalent to $\lambda/4$. This makes its clear that thicker the material, the better absorption for low frequencies.

- **Specific Flow resistance** R_f in (Nsm^{-3}) or MKS rayl is defined as the resistance offered by the material to flow of air through it.

$$R_f = \frac{\Delta P}{u} \tag{2.5}$$

  where ΔP is the pressure difference in ($\mathrm{Nm}^{-}2$) between either sides of the surfaces and u in ($\mathrm{ms}^{-}1$) is the particle velocity produced in the material. In general, the larger the flow resistance, the lower the absorption coefficient except at low frequencies where the situation is reversed.

- **Porosity** P of a material means the available volume of open pores. It is expressed in percentage [14].

$$P = \frac{volumeofporesconnectedtoexternalair}{totalvolume} \tag{2.6}$$

Based on the characteristic of a porous absorber, empirical models to determine the absorbers characteristic impedance Z_m and propagation constant k_m were developed. For this study, the focus will be on the model developed by M.E. Delany and E.N. Bazley [5] which is based on knowing the flow resistance of the material.

$$Z_m = \rho_o \cdot c_o[1 + 0.0571 \cdot E^{-0.754} - j \cdot 0.087E^{-0.732}] \tag{2.7}$$

$$k_m = k_o[1 + 0.0978 \cdot E^{-0.700} - j \cdot 0.189E^{-0.595}] \tag{2.8}$$

$$E = \frac{\rho_o \cdot f}{\sigma} \tag{2.9}$$

where σ is the flow resistivity, ρ_o is the air density, c_o is the speed of sound in air, k_o is the wave number in air and f is the wave frequency.

2.2.2 Characteristics of Resonator panel absorbers

For this study, the focus will be on resonator panels such as micro perforated panels which combine the physics of the resonator and panel absorbers. A micro-perforated panel (MPP) consists of a thin sheet panel perforated with a lattice of sub-millimetre apertures which create high acoustic resistance and low acoustic mass reactance necessary for broadband sound absorption without further using additional porous material [17]. The working of a MPP absorption is basically the same as ordinary perforated panels. Therefore, an MPP is used in the same way as ordinary perforated panels: placed parallel with a rigid back wall and an air-back cavity in between, as in seen in figure(2). However, with perforations smaller than a millimetre, MPPs can produce an acoustic resistance around $\rho_o c_o$, which is optimal to obtain high absorption[14].

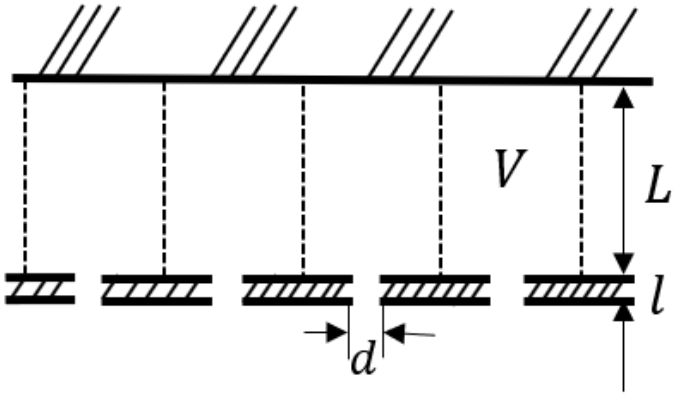

Figure 2: Construction of a micro perforated panel

The pioneer in the development of MPP and predicting the formulas for acoustic resistance and reactance is Dah-You Maa[12].

$$r = \frac{32\eta \cdot t}{p \cdot \rho_o c_o \cdot d^2}\left(\sqrt{1 + \frac{x^2}{32}} + \frac{\sqrt{2} \cdot x \cdot d}{32 \cdot t}\right) \tag{2.10}$$

$$\omega m = \frac{\omega \cdot t}{p \cdot c_o}\left(1 + \frac{1}{\sqrt{1 + \frac{x^2}{2}}} + 0.85\frac{d}{t}\right) \tag{2.11}$$

where x, called the perforate constant is given by

$$x = \frac{d}{2} \cdot \sqrt{\frac{\rho_o \omega}{\eta}} \tag{2.12}$$

p, called the perforation ratio is given by

$$p = \frac{\pi}{4} \cdot \frac{d^2}{b^2} \tag{2.13}$$

and r is the acoustic resistance, ωm is the acoustic reactance, d, b and t are the hole diameter, distance between the holes and panel thickness of an MPP, respectively. η is $17.9 \cdot 10^{-6}$ Pa is the coefficient of the viscosity of air. The characteristic impedance Z_{mpp} of the MPP is as follows:

$$Z_{mpp} = r + j\omega m \tag{2.14}$$

The parameters which define the behaviour and performance of a MPP are the perforation constant x and the acoustic resistance r. In general, perforated panels with hole size in millimeter or centimeter provide low acoustic resistance and hence the diameter size when reduced to sub-millimeter provided inherently better acoustic resistance and low mass reactance. The perforation constant as seen in 2.12 depends on d and $\sqrt{\omega}$. As the value of x increase the acoustic resistance increase, contributing to better absorption[13].

2.3 Reflection factor,Absorption coefficient and wall impedance

For the case of a plane wave hitting boundary wall as seen in figure(3), one can define and understand the relation between reflection coefficient , absorption coefficient and wall impedance by following[23].
The reflection factor from 2.3 can be further defined by the intensities in the two waves. As the intensity is plane wave is proportional to the sound pressure squared, the reflection factor becomes $|R_p|^2$ and part of the energy lost in the reflection process is $1 - |R_p^2|$, which is nothing but the absorption factor/coefficient.

$$\alpha = 1 - |R_p|^2 \tag{2.15}$$

Wall impedance Z_g at the surface is defined by:

$$Z_g = \frac{p}{v_n} \tag{2.16}$$

where v_n is the particle velocity normal to the wall and p is the pressure difference on either side of the wall. Finally R_p from the below figure can be defined as

$$R_p = \frac{Z_g \cos\phi - Z_o}{Z_g \cos\phi + Z_o} \tag{2.17}$$

Or in terns of Z_g

$$Z_g = \frac{Z_o}{\cos\phi} \cdot \frac{1 + R_p}{1 - R_p} \tag{2.18}$$

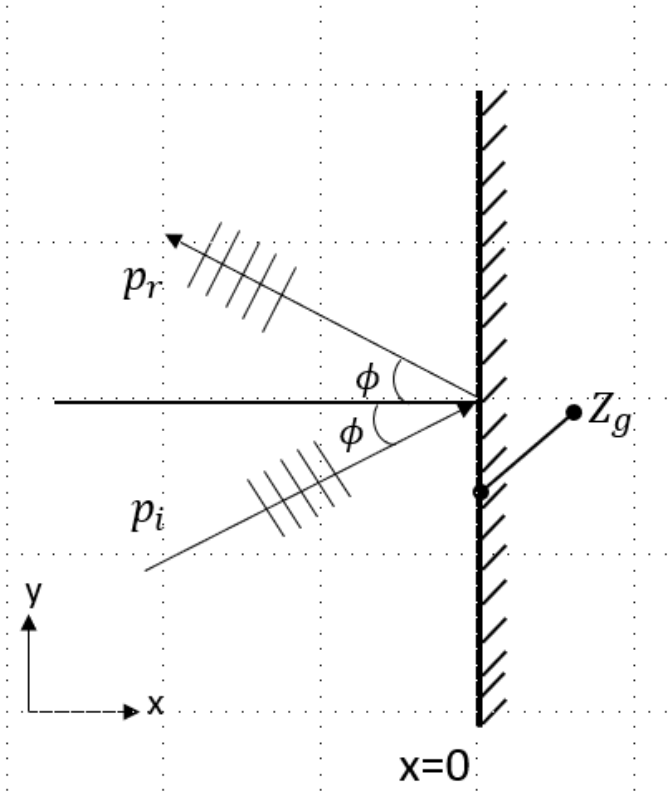

Figure 3: Sound incidence at an angle ϕ on a locally reacting boundary of impedance Z_g

Inserting 2.17 into 2.15, one can obtain the absorption coefficient of the boundary/wall as

$$\alpha_\phi = 1 - |\frac{Z_g \cos\phi - Z_o}{Z_g \cos\phi + Z_o}|^2 \tag{2.19}$$

Now, if the wall is shifted by a distance d with respect to the reference plane x, an air-gap which acts like a cushion is formed as seen in figure(4). As a consequence of this, the reflected wave has to travel twice the distance of d before it arrives again to the initial position of the reference plane while the absorption factor remains unchanged since there is no physical changes.

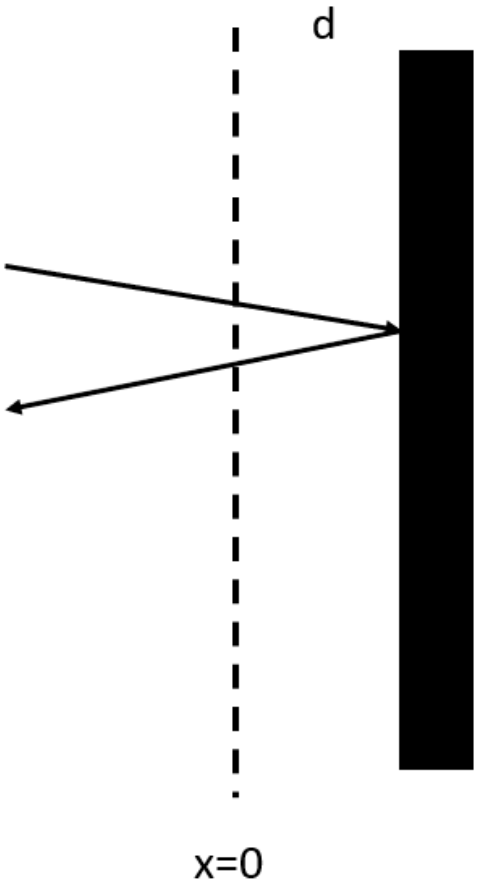

Figure 4: Shift in reference plane x

Following [10], the reflection factor of the reference plane is

$$R_p = \exp\left(-2jk_o d\right) \tag{2.20}$$

and the impedance Z_g as per eq. 2.18 is

$$Z_g = \frac{Z_o}{\cos\phi} \cdot \frac{1 + \exp\left(-2jk_o d\right)}{1 - \exp\left(-2jk_o d\right)} = -jZ_o \cdot \cot(k_o d) \tag{2.21}$$

Eq.2.21 is the wall impedance of a layer of air backed by a hard wall/boundary.

If we imagine the air-gap of thickness replaced by a porous absorber under similar conditions, the above equation is modified as

$$Z_{pm} = -jZ_m \cdot \cot k_m d \tag{2.22}$$

where Z_{pm} is the acoustic impedance of the porous layer backed by a hard wall/boundary. Similarly, for the case of a MPP backed with an air-gap depth of d to the wall as per [12] is given as

$$Z_{mpp} = r + j\omega m - jZ_o \cdot \cot(k_o d) \tag{2.23}$$

2.4 Transfer Matrix Method

The transfer matrix method is a fast analytical tool used to describe wave propagation in periodic structures such as porous or fluid layers. This model is usually applied to one-dimensional problems and in the case of acoustics, it can used to determine parameters in structures/layers such as effective wavelength k_{eff} and effective characteristic impedance Z_{eff} [8].

For a single layer of homogeneous material the relation between the acoustic magnitudes evaluated at the boundaries as shown in figure(5).

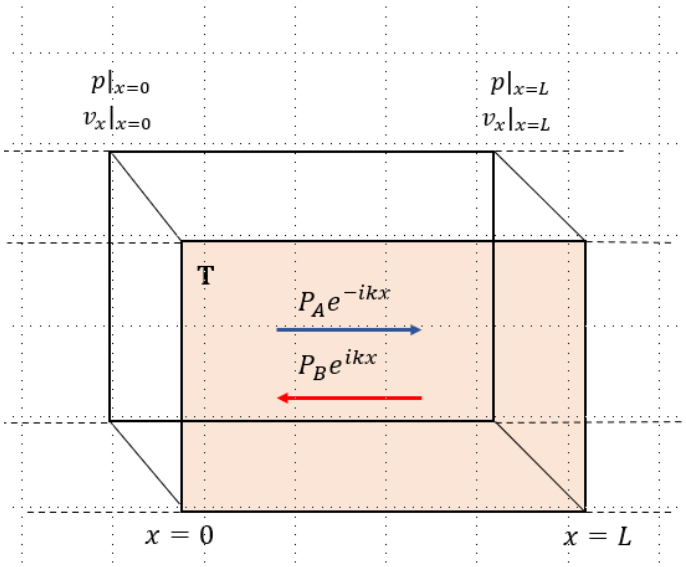

Figure 5: Acoustic material characterised by transfer matrix **T** with wave propagation modelled inside the material

From the above figure, an assumption of longitudinal plane wave in the layer with a harmonic dependence of $e^{j\omega t}$, the total acoustic field can be described as a superposition of two waves propagating in opposite directions.

$$p(x) = P_A \cdot e^{-jkx} + P_B \cdot e^{jkx} \tag{2.24}$$

$$v(x) = \frac{P_A}{Z_o} \cdot e^{-jkx} - \frac{P_B}{Z_o} \cdot e^{jkx} \tag{2.25}$$

After applying boundary conditions at either side of the 1D layer, the acoustic magnitudes can be related as a 2×2 matrix which depends on the impedance and wave number of the material.

$$\begin{bmatrix} p \\ v_x \end{bmatrix}_{x=o} = \begin{bmatrix} \cos(kL) & j \cdot Z \sin(kL) \\ j\frac{1}{Z}\sin(kL) & \cos(kL) \end{bmatrix} = \begin{bmatrix} p \\ v_x \end{bmatrix}_{x=L} \tag{2.26}$$

From the above equation the total transfer matrix **T** is defined by relating the sound pressure p and normal velocity v_x at the beginning $x = 0$ and at the end of the structure $x = L$ as

$$\begin{bmatrix} p \\ v_x \end{bmatrix}_{x=o} = \mathbf{T} \begin{bmatrix} p \\ v_x \end{bmatrix}_{x=L} \tag{2.27}$$

where the total transfer matrix $\mathbf{T}$ is a 2×2 matrix as

$$\begin{bmatrix} p \\ v_x \end{bmatrix}_{x=o} = \begin{bmatrix} T_{11} & T_{12} \\ T_{21} & T_{22} \end{bmatrix} \begin{bmatrix} p \\ v_x \end{bmatrix}_{x=L} \tag{2.28}$$

For a structure composed of several layers as shown in figure(6), the total transfer matrix $\mathbf{T}$ is given by the product of the transfer matrices of each layer i.e $\mathbf{T}= T_1 \cdot T_2 \cdot T_3$

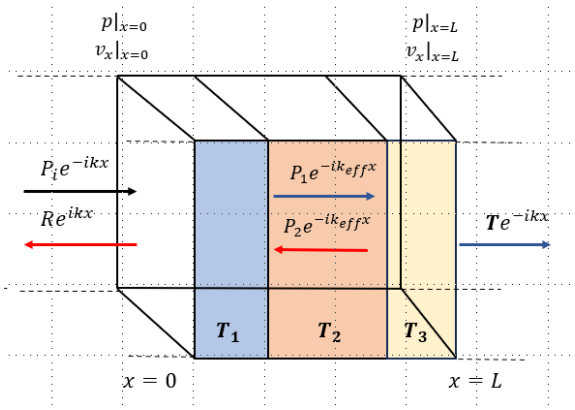

Figure 6: Acoustic structure composed of several layers of effective parameters,((After, Noé Jiménez, Jean-Philippe Groby, and Vicent Romero-Garcíaet, *The Transfer Matrix Method in Acoustics*,p107,2021))

$$T = \prod_{n=1}^{N} T_n \tag{2.29}$$

Through the total transfer matrix $\mathbf{T}$, various information of the system can be obtained, such as the effective impedance and wave-number.

For the case of a symmetric structure , the total transfer matrix can be modelled as an equivalent one dimensional fluid-like layer with complex and frequency dependent effective parameters. Thus the total transfer matrix for an effective length of L is

$$\mathbf{T} = \begin{bmatrix} T_{11} & T_{12} \\ T_{21} & T_{22} \end{bmatrix} = \begin{bmatrix} \cos(k_{eff}L) & j \cdot Z_{eff} \sin(k_{eff}L) \\ j\frac{1}{Z_{eff}} \sin(k_{eff}L) & \cos(k_{eff}L) \end{bmatrix} \tag{2.30}$$

- Effective Wave-number, from eq 2.28 and 2.30 one can obtain the expression for the effective wave-number as a coefficient of the total transfer matrix

$$k_{eff} = \frac{1}{L} \cos^{-1}\left(\frac{T_{11} + T_{22}}{2}\right) + \frac{n\pi}{L} \tag{2.31}$$

- Effective characteristic impedance can also be obtained from the total transfer matrix coefficients as

$$Z_{eff} = \sqrt{\frac{T_{12}}{T_{21}}} \tag{2.32}$$

2.5 Prediction of Sound absorption Coefficient

So far the sound absorption coefficient was deduced for normal incidence α and incidence for a particular angle of interest α_ϕ , from eq 2.15 and 2.19 respectively, on the assumption of a locally reacting surface. As per 2.4, the complex effective characteristic impedance Z_{eff} obtained can applied to eq 2.19 resulting in

$$\alpha_\phi = \frac{4 \cdot Re(Z_{eff}) \cos\phi}{(Re(Z_{eff}) \cos\phi + 1)^2 + (Im(Z_{eff}) \cos\phi)^2} \tag{2.33}$$

But, the average of the absorption coefficient for different angle of incidence is of practical interest and this is called statistical absorption coefficient α_s, as described by E.T Paris[15]. Also called the Paris formula.

$$\alpha_s = 2 \int_0^{\frac{\pi}{2}} \alpha_\phi \sin\phi \cos\phi d\phi \tag{2.34}$$

However, from [22], the impact of finite size vs infinite size of the absorber was discussed. S.I Thomasson proposed the angle dependent absorption coefficient of infinite locally reacting material with impedance Z_A as

$$\alpha_\infty(\phi) = 4 \cdot \frac{\frac{Re(Z_A)}{\cos\phi}}{|Z_A + \frac{1}{\cos\phi}|^2} \tag{2.35}$$

An extension of the theory for finite case as

$$\alpha(\phi) = 4 \cdot \frac{Re(Z_A) Re(Z_f)}{|Z_A + Z_f|^2} \tag{2.36}$$

where Z_f is the field/radiation impedance of the absorber which depends on the area of the sample S in question and for the use in this thesis a simplified approach is used, as per [18]

$$Z_f = -\frac{ik}{2\pi S} \int_0^a \int_0^b 4 \cdot \cos(k_x \kappa) \cos(k_y \tau) \frac{e^{-ik\sqrt{\kappa^2+\tau^2}}}{\sqrt{\kappa^2+\tau^2}} (a-\kappa)(b-\tau) d\kappa d\tau \tag{2.37}$$

Furthermore in [22], the statistical absorption coefficient α_{stat} for a finite size absorber based on "maximum available power" over the "incident projected power" is given as

$$\alpha_{stat} = 4 \cdot Re(Z_A) \cdot \frac{\int_0^{\frac{\pi}{2}} \int_0^{2\pi} \frac{\sin\phi}{|Z_A+Z_f|^2} d\phi d\theta}{K} \tag{2.38}$$

where K is

$$K = \frac{1}{\pi} \int_0^{\frac{\pi}{2}} \int_0^{2\pi} \frac{\sin\phi}{Re(Z_f)} d\phi d\theta \tag{2.39}$$

The implication of considering the size of the absorber lies in measurement of sound absorption coefficient. The random incidence sound absorption coefficient is measured as per ISO 354 [7] in a reverberation chamber, with requirements for the sample size to be larger than $10\,\mathrm{m}^2$ for a specified volume of the room. For instance, if the sample size is much smaller than mentioned, the measured value increases and at times exceeding the value of 1 [23]. This is due to the phenomenon called the *Area or Edge effect* As explained in [14] and [23], the *edge effect* is caused by the diffraction of incident sound waves around the absorptive material. This is the case when the linear dimension of the sample is smaller than the acoustic wave-length leading to the apparent larger acoustical area or greater absorption which is not true in reality.

With the measurement method ISO 354 Acoustics – Measurement of sound absorption in a reverberation room [7], the measurement is considered under diffuse sound field conditions but for non-diffuse sound field or free-field conditions one has to consider **in-situ measurement methods**. The most well accepted method and which is of interest in this study is the temporal subtraction method as explained in [3] and ISO 13472-1[1]. The method is based on impulse measurements taken above the surface of the sample using a single microphone and the resulting transfer function between the output of the signal generator and the microphone. The transfer function consists of two factors, one from the direct path(signal generator to loudspeaker to microphone) and reflected path(signal generator, loudspeaker and surface under test to the microphone)(see figure(7)).

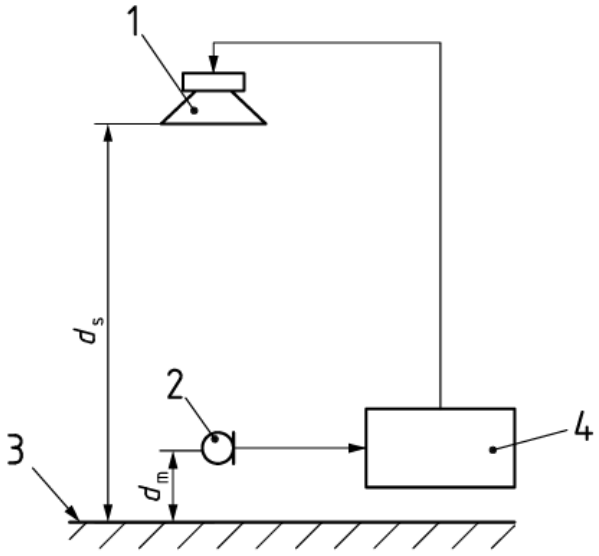

Figure 7: Measurement setup as described in *SS-ISO 13472:1*

Keys:
1: Directed loudspeaker
2: Free-field omni direction microphone
3: Test sample
4: Signal generator
d_s is the distance between loudspeaker and reference plane for the test sample.
d_m is the distance between microphone and reference plane for the test sample.

Thus the overall impulse in time domain consists of the direct signal response and after a little delay, the reflected signal response.

With time domain signal processing and signal separation procedure as seen in figure(8), the two responses are separated. Post Fourier transform, the transfer function of the direct path $H_i(f)$ and reflected path $H_r(f)$ are obtained. The squared modulus of these transfer function gives the sound power reflection factor $Q_w(f)$ and in order to account for the geometrical spreading due to difference in path length between the direct and reflected sound, a factor called the geometrical factor K_r is multiplied to the sound power reflection factor. Then the sound absorption coefficient can be found as

$$\alpha(f) = 1 - Q_w(f) = 1 - \frac{1}{K_r^2} \cdot |\frac{H_r(f)}{H_i(f)}|^2 \tag{2.40}$$

$$K_r = \frac{d_s - d_m}{d_s + d_m} \tag{2.41}$$

the transfer function of the reflection coefficient is obtained which is used to determine the absorption coefficient.

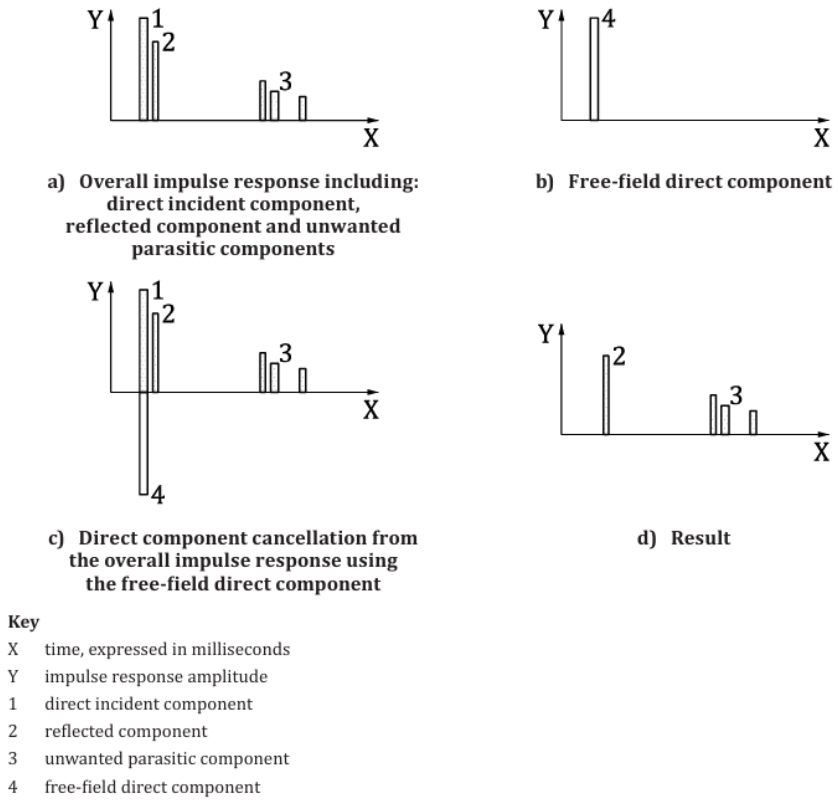

Figure 8: Signal separation procedure as described in *SS-ISO 13472-1*

3

Methods

This section describes the criteria for the selection of the absorber system, its theoretical modelling and absorber parameter analysis. Further, the measurement method of the absorption coefficient for the said absorber in diffuse and free-field conditions are explained. Lastly, the equipment used is listed.

3.1 Determining the absorber system

The selection of the absorber system was based on the sound field behaviour in corridors and its placement in typical middle schools. For the latter part, a non traditional approach was considered, i.e, using furniture which acted as storage spaces along the length of the corridor, to mount the abosrber. The purpose of this was to utilize the space on the surface of the furniture and reduce additional absorber installations. *Efterlang*, with whom this thesis was collaborated with suggested one of the following designs as seen in figure(1) for a typical furniture used in school corridors. Based on which, the dimensions of 300 mm× 398 mm were considered for the fabrication. Additionally, for pragmatic reasons the thickness of the system was aimed to be kept under 25 mm.

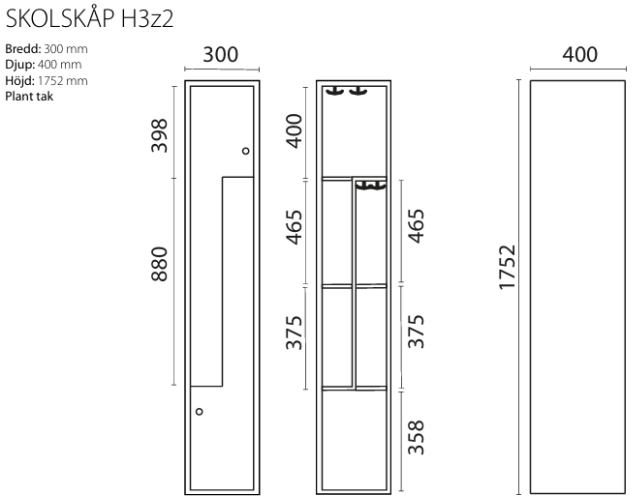

Figure 1: Suggested reference for the considered furniture design, from SONESSON INREDNINGAR,After,*https://www.sonesson.se/sortiment/skolskaap-elevskaap/skolskap-elevskap-h3z2.html*)

For the working frequency range of the sound absorber, Swedish building regulations[21], ISO 717-1:2020[6] and SS 25268:2023[2] were studied and an operating range of 150 Hz − 4000 Hz was found to be the focus of their attention. However, due to the size of the absorber defined, frequencies below 850 Hz was not considered since the linear dimension of the absorber is smaller than the the wavelength of the incident sound wave in air, leading to diffraction and over estimation of absorption. Hence the focus of the working range was decided as 850 Hz − 4000 Hz.

With the size and operating frequency range defined, the next step is to optimize the absorber system based on the type of absorber as discussed in 2.2. A broad-band resonant absorber was considered, consisting of micro-perforated panel, air-gap and porous material, with a resonant frequency at 2000 Hz and this was to consider the impact of high frequency noise and to improve the perceived intelligibility[4].

3.2 Theoretical modelling

Design of the absorber system with its individual components was modelled in Matlab software for a resonant peak at 2000 Hz to find the sound absorption coefficient. Under the assumption of a locally reacting material, the characteristic impedance of the individual components was determined and using TMM the effective characteristic is calculated as mentioned in 2.4. For a the porous material, as per eq 2.27, the transfer matrix for a porous material T_p is given as

$$T_p = \begin{bmatrix} \cos(k_m L_m) & j \cdot Z_m \sin(k_m L_m) \\ j\frac{1}{Z_m}\sin(k_m L_m) & \cos(k_m L_m) \end{bmatrix} \tag{3.1}$$

where Z_m and k_m are the characteristic effective impedance and wave-number of the porous material and can be calculated from eq 2.7 to 2.9.
For an air-gap, the transfer matrix T_o is given as

$$T_o = \begin{bmatrix} \cos(k_o L_o) & j \cdot Z_o \sin(k_o L_o) \\ j\frac{1}{Z_o}\sin(k_o L_o) & \cos(k_o L_o) \end{bmatrix} \tag{3.2}$$

where Z_o and k_o are the characteristic impedance and wave-number of air.
Lastly, for the micro-perforated panel the transfer matrix T_{mpp} is given as [23]

$$T_{mpp} = \begin{bmatrix} 1 & Z_{mpp} \\ 0 & 1 \end{bmatrix} \tag{3.3}$$

The total transfer matrix $\mathbf{T}$ is given as

$$\mathbf{T} = T_p \cdot T_o \cdot T_{mpp} \tag{3.4}$$

Using the above equation Z_{eff} is found as per eq 2.32 and subsequently the resulting absorption coefficient for normal incidence and incident angles between 0 deg-90 deg in steps of 10 deg is found using eq 2.33. Lastly, the statistical absorption coefficient for finite and infinite case is determined.

3.2.1 Parameter Analysis

Parameters which affect the absorption coefficient for the absorber system are investigated with different values:

- **Flow resistivity and thickness of the porous absorber** As discussed in 2.2.1,flow resistivity and thickness go hand in hand.
  For the case porous material thickness, from the figure (2), a reduction in material thickness of 13 mm leads to shift in the peak resonance frequency and an over decrease in absorption coefficient for different incident angles and random incidence while an increase in thickness leads to an over increase in absorption coefficient and a noticeable change in the high frequency region. This can be attributed to the increase in path length.

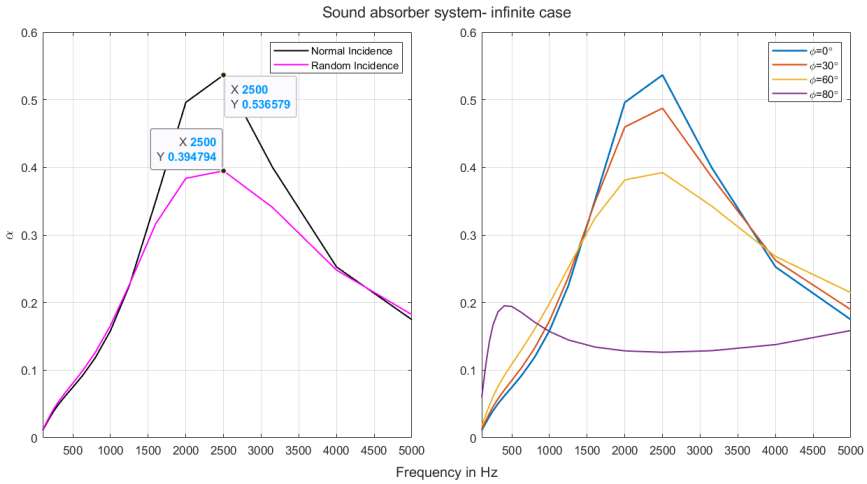

(a) Porous material with a thickness of 13 mm

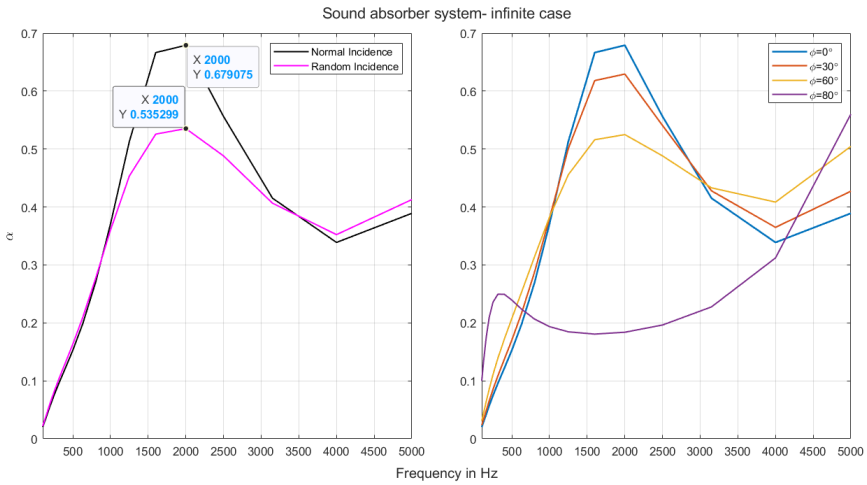

(b) Porous material with a thickness of 22 mm

Figure 2: Absorption coefficient for changes in Porous absorber material thickness

While from figure (3), it can be deduced that an increase in flow resistivity leads to an higher absorption coefficient. The opposite holds true for the case of reduced flow resistivity.
Interestingly, with an increase in flow resistivity, sound attenuation improves in the material but it also leads to an increase in impedance leading a reflected wave. While a lower flow resistivity does reduce the impedance of the material but the rate of attenuation also decreases. Both cases can be improved with an apt material thickness,

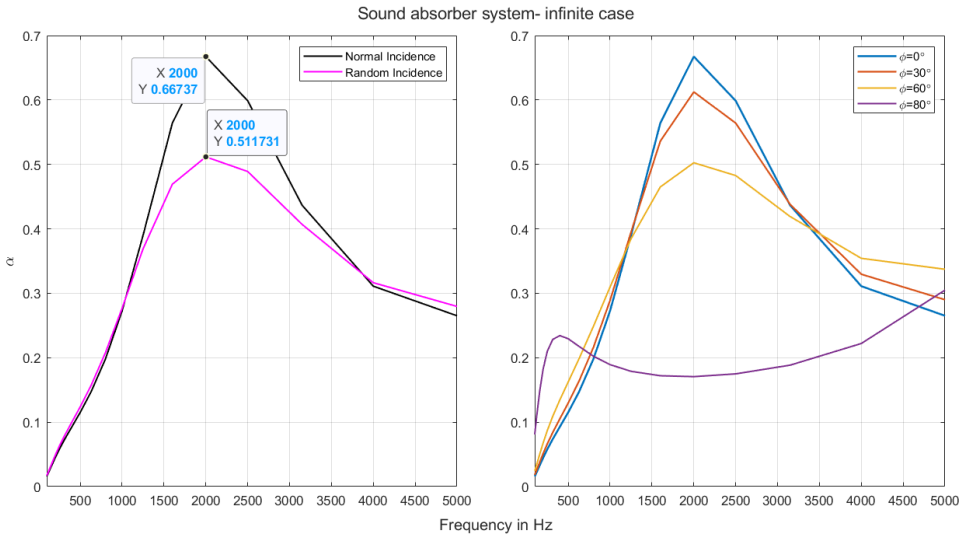

(a) Porous material with a flow resistivity of $15\,000\,\mathrm{Nsm}^{-3}$

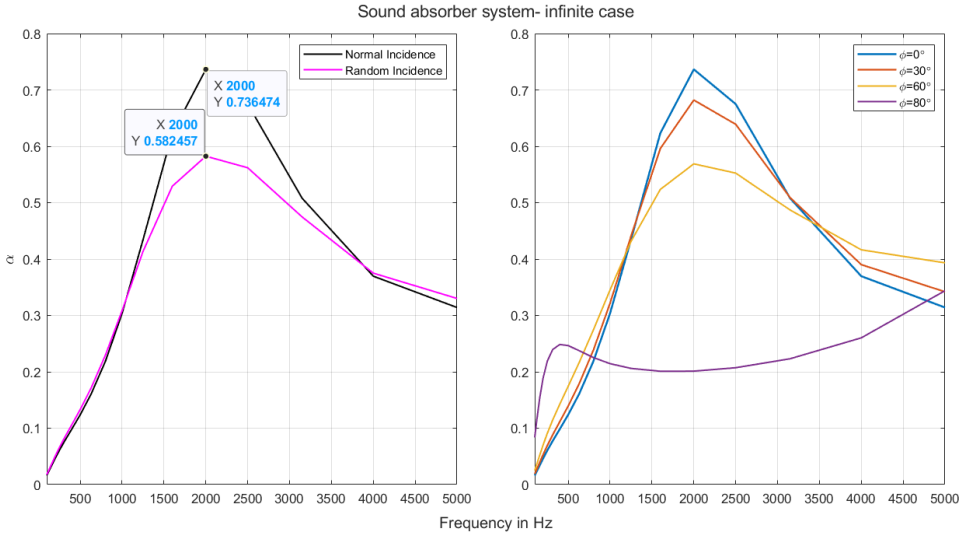

(b) Porous material with a flow resistivity of $20\,600\,\mathrm{Nsm}^{-3}$

Figure 3: Absorption coefficient for changes in flow resistivity

- **Effect of air-gap** An increase in air-gap is generally associated with an increase in absorption coefficient due to an increase in effective path length and better impedance matching. But in figure (4), an increase of 8 mm leads to an overall decrease in absorption coefficient but an improvement in the high frequency region while a reduction in air-gap of 2 mm showed an improvement in the overall absorption coefficient. This contradiction can be attributed to the creation of destructive interference in the air cavity region and the change in path length in the incident and reflected wave.

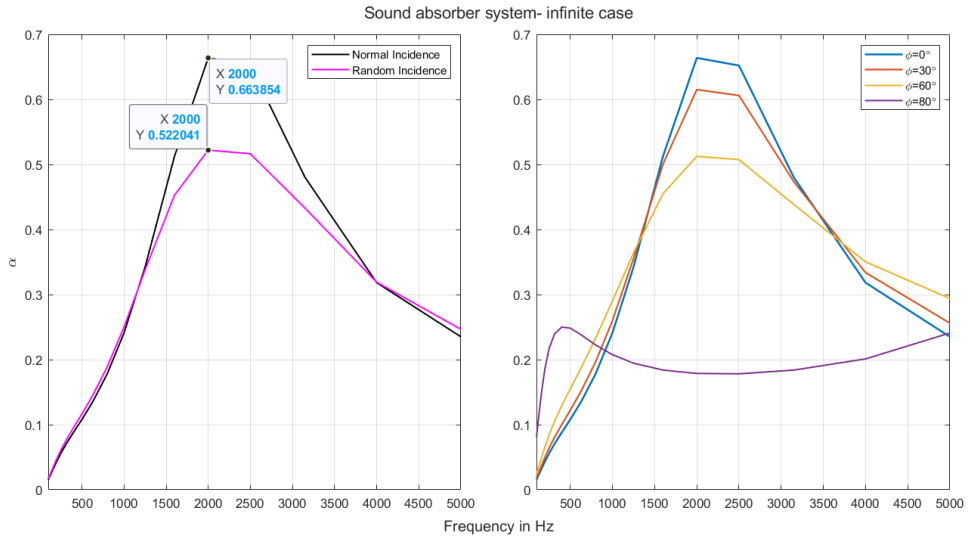

(a) Air-gap of 2 mm

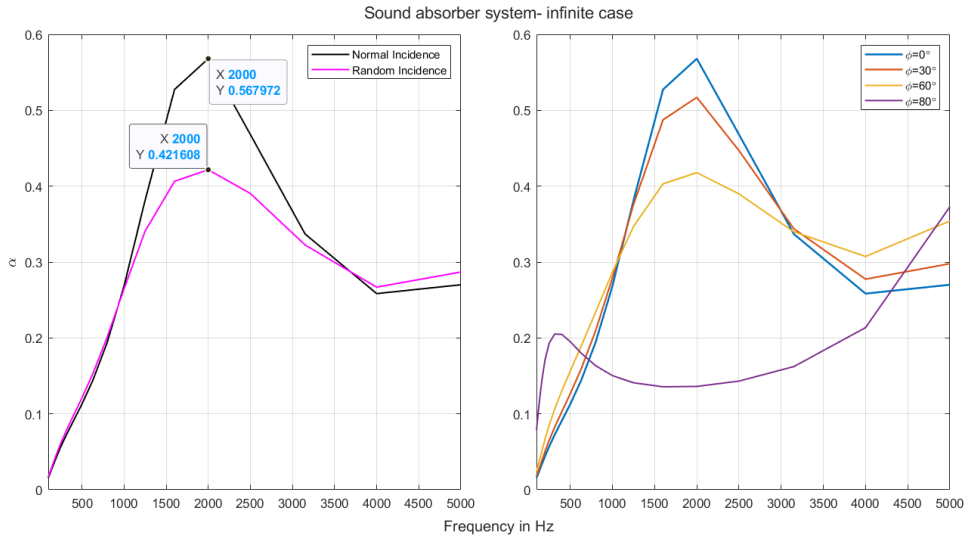

(b) Air-gap of 8 mm

Figure 4: Absorption coefficient for changes in Air-gap width

- **Perforation constant** From 2.2.2, the perforation constant x is dependent on the hole diameter (d) and appropriate values of perforation ratio (p) which is decided by the distance between the holes and area of the surface. Figure (5 and 6) shows investigative results for changes in hole diameter and distance between hole. For d =1.25 mm, from figure (5), an overall increase in absorption coefficient is seen, however a shift in resonance peak followed by a narrower bandwidth is observed while for an increase of d =2 mm, the overall absorption coefficient decreases while the peak shifts moves towards higher frequencies and the bandwidth increases. These changes are governed by the acoustic resistance offered by the hole, which is more when the hole diameter decreases and the shift in frequency is due to the behaviour of the holes as Helmholtz resonators.

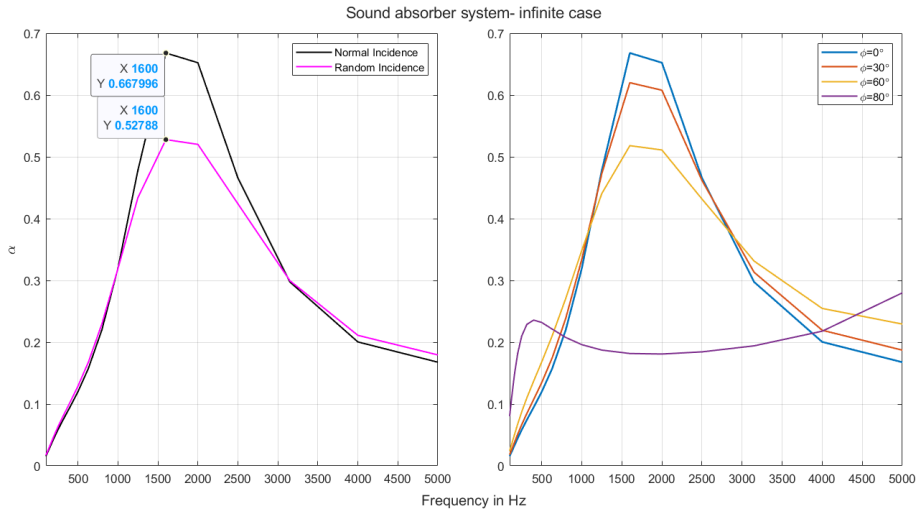

(a) Micro perforated panel of d=1.25 mm

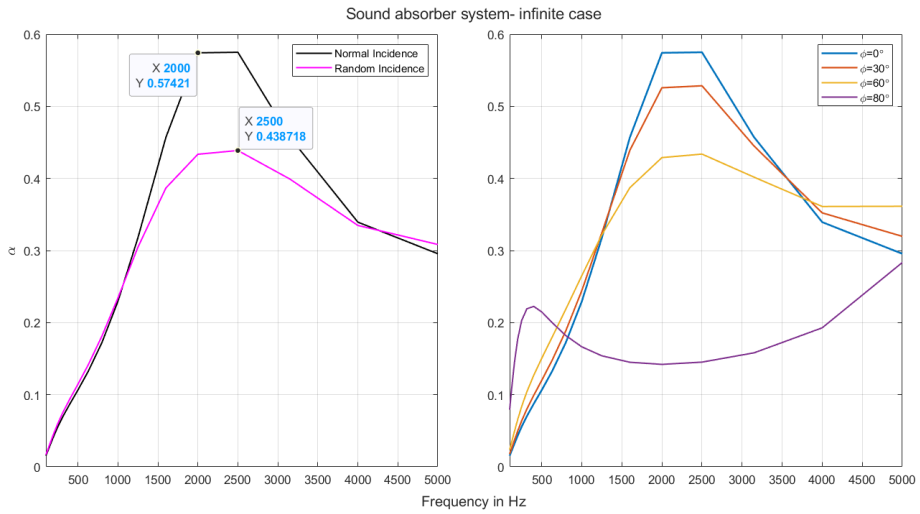

(b) Micro perforated panel of d=2 mm

Figure 5: Absorption coefficient for changes hole diameter

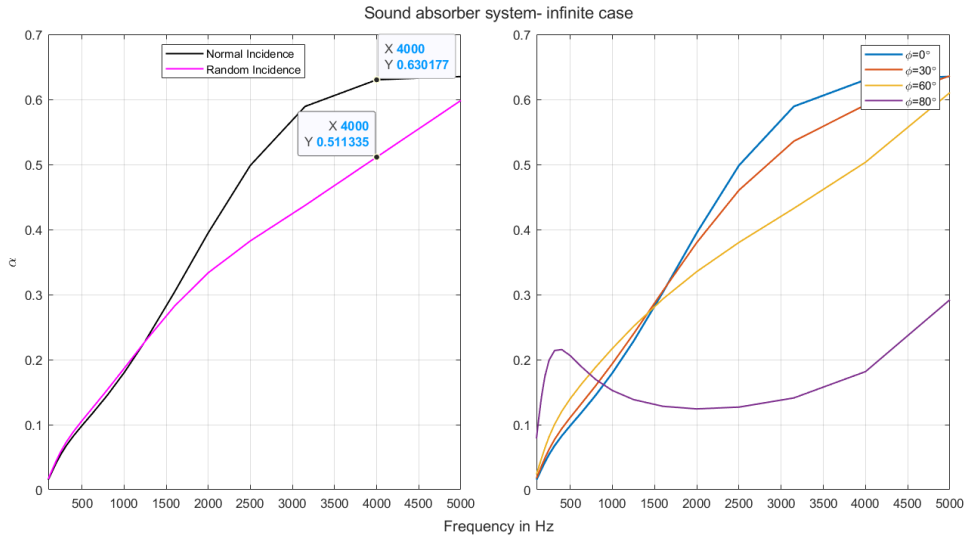

(a) Micro perforated panel of b=2 mm

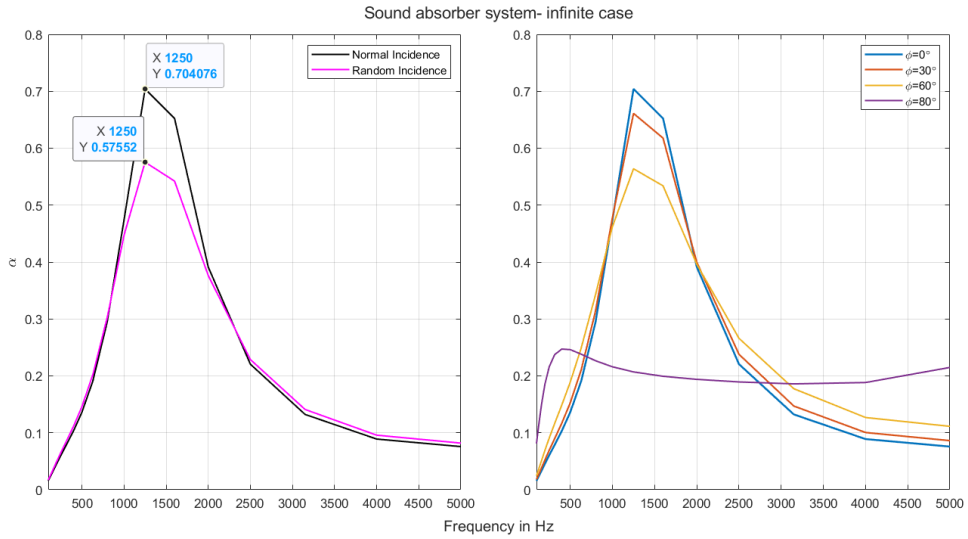

(b) Micro perforated panel of b=8 mm

Figure 6: Absorption coefficient for changes in distance between holes

From figure (6), smaller values for b means higher density of holes per unit area leading to more interaction between the panel and sound waves and an increase in the sound absorption coefficient, particularly in the mid-higher frequency region. But, the resonance is peak is lowered. While for larger values of b, the overall sound absorption increases and resonance peaks shifts to lower frequency, contrary to expectation.

3.2.1.0.1 Key take aways

- Smaller values of flow resistivity can be over come with thicker material.
- Large air gap doesn't equate to better absorption due to possibility of destructive interference since the path length increases.
- Small hole diameter impacts the acoustic resistance offered. Direct impact on high frequencies.
- With a larger hole size, high frequency absorption reduces since the panel might behave like a transparent medium.
- Lower perforation ratio improves acoustic resistance
- Narrow bandwidth is an indicator of better coupling. Like a Helmholtz resonator.

3.3 Experimental Validation

To find the absorption coefficient of the fabricated absorber system, two sets of measurement were carried out.

3.3.1 Measurement method 1

The primary measurement was to find the statistical absorption coefficient and the procedure was as per ISO 354[7]. The reverberation chamber at the department of Sound and Vibration at Chalmers University of Technology was used to conduct the measurement as seen in figure(7).

Figure 7: Measurement setup in the reverberation chamber.

It has a volume of 96.6 m^3. During the experiment, an omni-directional speaker sent out pink noise and the sound was measured in three different source-receiver positions. Two different loudspeaker position with three different microphone positions each. Thus a total of 6 measurements. The omni-directional diffuse field microphones used were at least 1.5 m apart, 2 m from the loudspeaker and 1 m from any room surface and the test specimen. Through the interrupted noise method, the number of repetitions at each microphone position was three and the time per repetition was 10 s with a sampling frequency of 25 600 Hz

The decay curves captured was later used to process the reverberation times, from which the equivalent absorption area and the absorption coefficient was calculated.

3.3.2 Measurement method 2

The next set of measurements was as per SS-ISO 13472:1 i.e acoustic measurement of sound sound absorption properties of road surface in situ- Part 1:extended surface method[1]. This was done to observe the behaviour of the fabricated absorber system in conditions were diffuse field was absent and to understand the behaviour of sound incident angle.

The setup was as per figure(7) and the location for the setup is seen below. The noise barrier seen in the figure was chosen to provide a large reflecting surface and as a substitute for a wall/ground surface since there was challenges in mounting the speaker. d_s and d_m were chosen as per the standard, i.e 1.25 m and 0.25 m respectively. The directional loudspeaker sent a broad band signal and the impulse response consisting of direct and reflected signals is captured at the microphone with a sampling frequency of 51.2 kHz. With the same geometrical specification, the direct signal impulse is captured with-out the absober, which is used in signal separation. Further more, the same setup is utilised to find the impact of incident angle. Eq 2.41 is modified as

$$K_{r,\theta}^2 = 1 - \cos^2\theta \cdot (1 - K_r^2) \tag{3.5}$$

Angles of 30 deg, 45 deg and 60 deg were investigated. The captured impulses responses are further computed in MATLAB software to find the absorption coefficient.

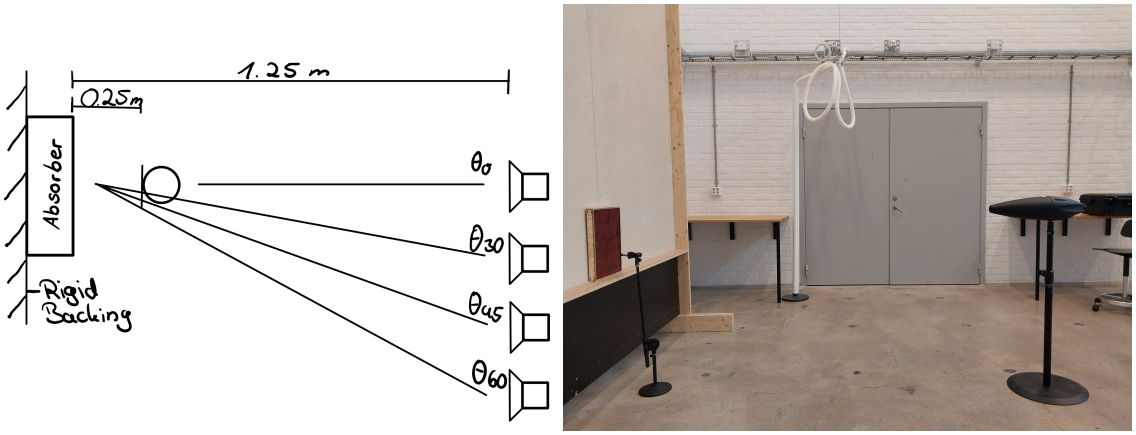

(a) Schematic representation **(b)** Side view

Figure 8: Free field setup for measurement method 2

3.4 List of equipment

The below equipment was sourced from Technical Akustik department of Chalmers University of Technology.

3.4.1 Measurement method 1

- An in-house omnidirectional speaker is used with an XLR input and BNC output.
- Agilent 33120A Signal generator for broad-band noise.
- Diffuse field microphones: GRAS 446AQ with serial number 488122, 488116 and 488117.
- Respective cables and microphone stands

3.4.2 Measurement method 2

- Omnidirectional loudspeaker, Brüel and Kjær Type 4295, Serial No. 2879487.
- Amplifier, Brüel and Kjær, Type 2735, Serial No. 2735-100389.
- Agilent 33120A Signal generator for broad-band noise.
- Omni-directional Free-field microphones: GRAS 146AE with serial number 474130.
- Respective cables and microphone stands

4

Results and Discussion

In this section, the results for theoretical modelling and fabrication are presented and discussed. Subsequently, the measurement results for method 1 and 2 are discussed.

4.1 Theoretical validation

Having a target of 2 kHz as the resonance frequency of the system and a thickness of under 25 mm, post parameter analysis, the chosen parameters are as follows:

Micro perforated panel

- t=0.5 mm
- d=1.65 mm
- b=5 mm

AirGap

- L_o=5 mm

Porous absorber(Mineral Wool)

- R_f=5000 Nsm^{-3}
- L_m=17.5 mm

Fabrication was carried out in the Chalmers Fuse Workshop. The choice of material for the micro perforated panel was ABS plastic which in most cases is not the traditional choice(eg.steel, Aluminium etc) and the reason for this were

- For a metal sheet, to punch/drill holes of a small diameter was a challenge with the current equipment present at the workshop.
- At the time of fabrication there was a lack of traditional material for the required panel thickness.
- ABS, a type of plastic was sufficiently stiff for our current needs and punching holes via laser cutter was much easier and faster.

Figure 1: Chosen porous absorber from ISOLINA

As for the porous absorber,figure(1), the material selected was FLAX wool from ISOLINA, since this was readily available at the department of Technical Akustiks, Chalmers University and the value for flow resistivity was provided by ISOLINA. Post fabrication of the micro-perforated plate, the remaining components were held together by 1 cm plywood as seen in figure (2).

(a) Top view **(b)** Side view

Figure 2: Fabricated sound absorber

4.1.1 Infinite size Absorber

The results from the calculation of absorption coefficient are shown in figure (3). For normal incidence the absorption coefficient α_0 was close to 0.65 and statistical absorption α_{stat} was 0.47. The trend for both the curves are similar below 1 kHz and above 3.5 kHz while for random incidence, a slight increase in α was observed.

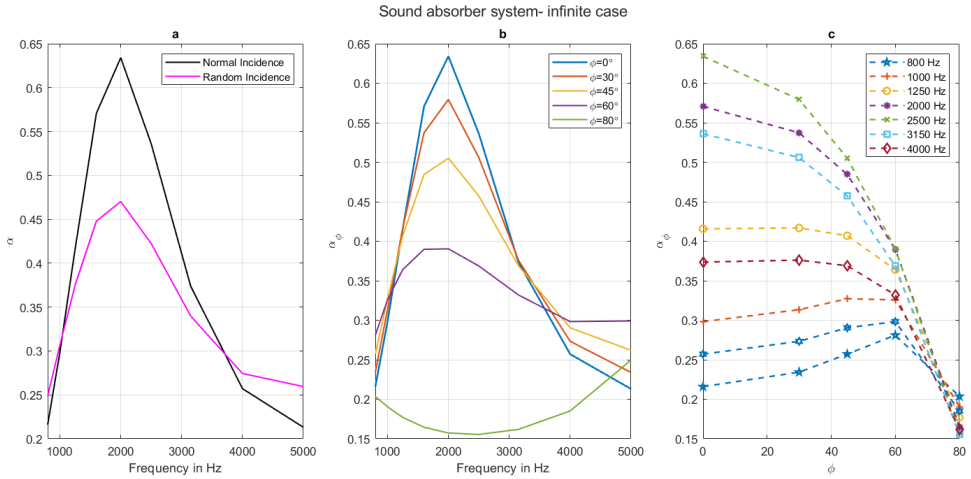

Figure 3: Absorption coefficient obtained by theoretical modelling of the absorber system for (a) Statistical vs normal incidence,(b) variation of angles and (c) certain frequencies over incident angles

This behaviour can be attributed for a few key reasons:

- **Energy distribution** for normal incidence, all the energy is found on a small area, leading to maximum interaction and resulting in more energy absorbed. In case of random incidence, the waves impinge in different direction of the absorber resulting in the spread of the energy thus reducing the intensity of interaction and lower absorption.
- **Reflection effect** There is lower complex reflection at normal incidence, resulting in less sound energy reflected while for random incidence or larger incident angle, the reflection factor is larger leading to lower absorption coefficient.
- **Absorber impedance**, at normal impedance, the impedance between the absorber and incident wave(in air) matches better while for random incident angles can cause a mismatch and reduce efficiency.

Continuing the analysis for infinite size absorber, the results for incident angles ϕ=0°, ϕ=30°,ϕ=60° and ϕ=80° are shown in figure(3). As ϕ increases α decreases and close to grazing incidence, the value tends to zero. This decrease is due to the shorter path length of the incident wave in the absorber system, leading to less interaction. Impedance mismatch increases along with higher reflection coefficient i.e more waves are reflected than absorbed. Thought the general behaviour follows the above reasoning, one can observe an increase in α at larger angles for high frequencies and this is attributed to the change in path length for different media encountered. From MPP to air gap to porous absorber. When observing the be-

haviour of frequencies over incident angles ascending from 0° to 90° in steps of 10°, the absorption coefficient is pronounced until 70° and drops drastically after.

4.1.2 Finite size absorber

The results from the calculation of absorption coefficient is shown in figure (4) based on eq 2.38. The absorption coefficient exceeding one is mainly due to the size of the absorber system i.e 0.1194 m^2.

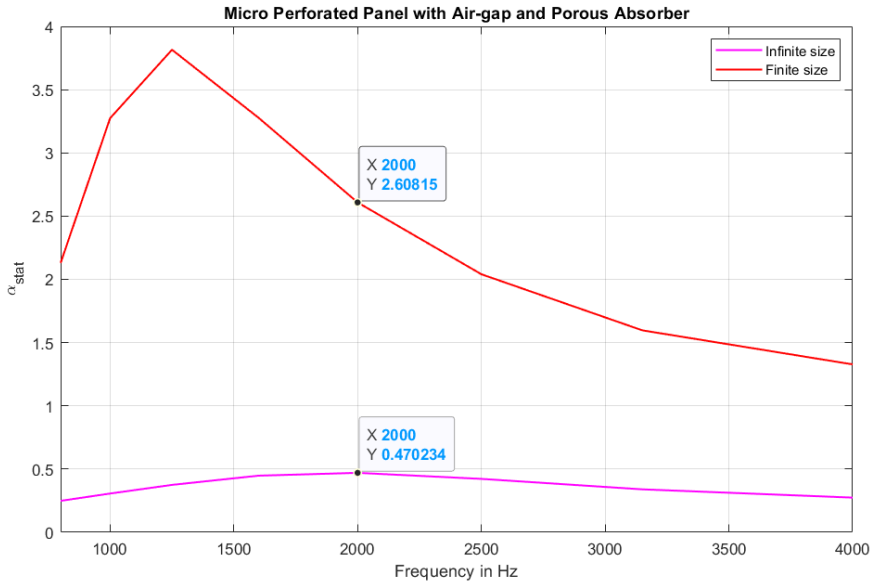

Figure 4: α_{stat} based on theoretical validation of a finite size absorber

To understand the behaviour of α_{stat}, lets observe the behaviour of angle of incidence on the absorption coefficient α_{ϕ}, along with individual frequencies over incident angles from the figure (5).

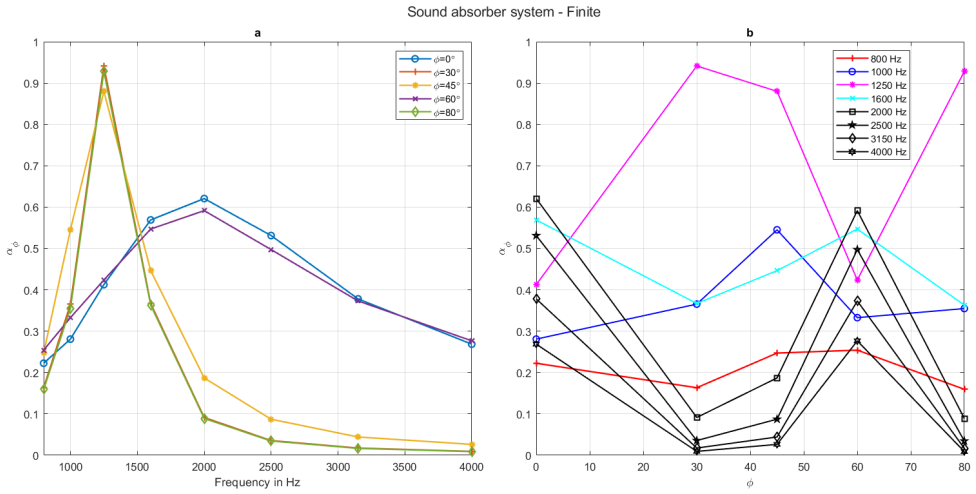

Figure 5: Absorption coefficient of finite size absorber seen with,a)incident angles b)individual frequencies of interest.

From the above figure, incident angles inspected are, 0°,30°,45°,60° and 80°. With angles 0° and 60° having peaks at 2 kHz and showing similar behaviour while for the remaining angles the peak has shifted to 1.25 kHz with larger absorption coefficient. However, the bandwidth is much narrower.
The aspect that is interesting is the fact that at 80° which is close to grazing incidence, frequencies between 800 Hz to 1600 Hz in (b) show absorption coefficient values greater than 0, which is contrary to the infinite absorber theory. This fact further supplements as to why α_{stat} values exceed 1.

4.2 Experimental validation

4.2.1 Measurement method 1

Following 3.3.1, the fabricated absorber system of surface area 0.1194 m^2 was measured for statistical sound absorption and the results are shown in figure (6). The general trend between the measured and calculated curves are similar but varying with the values of absorption coefficient at the resonance peak (1.25 kHz) and frequency of interest (2 kHz). Values over $\alpha_{stat} = 1$ were expected as mentioned in 2.5, due to the phenomenon of edge effect and deviations in the measurement procedure, i.e, size of the reverberation chamber and fabricated absorber being smaller than stateted by ISO 354.
Furthermore, from [22], the formula used to find the statistical absorption coefficient in ISO 354 is derived from Sabine[[7],eq (5)] which differs from eq 2.38 in terms of accounting for finite size of the absorber. Leading to much larger values of absorption coefficient.

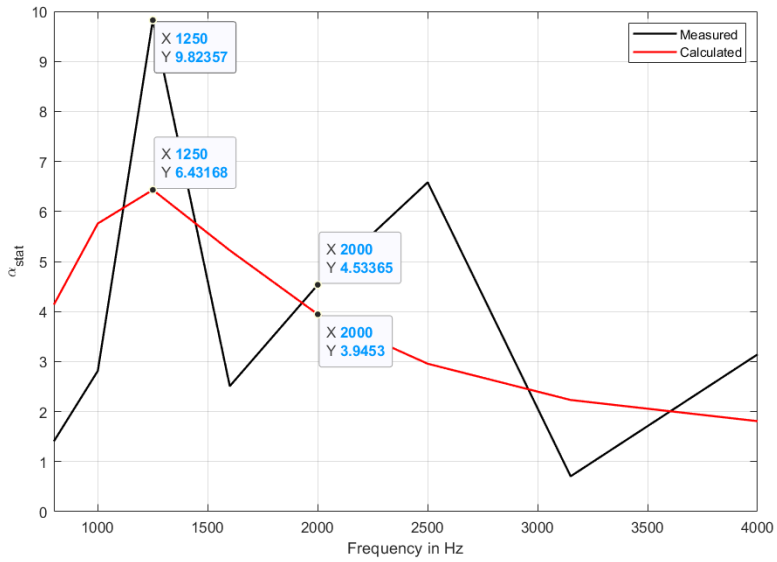

Figure 6: α_{stat} measured over 1/3 octave bands as per ISO 354 in a diffuse field for the fabricated sound absorber system and compared with theoretical calculation

4.2.2 Measurement method 2

Following 3.3.2, the incident angle dependent sound absorption coefficient for the fabricated absorber was measured and the results are shown in figure (7).

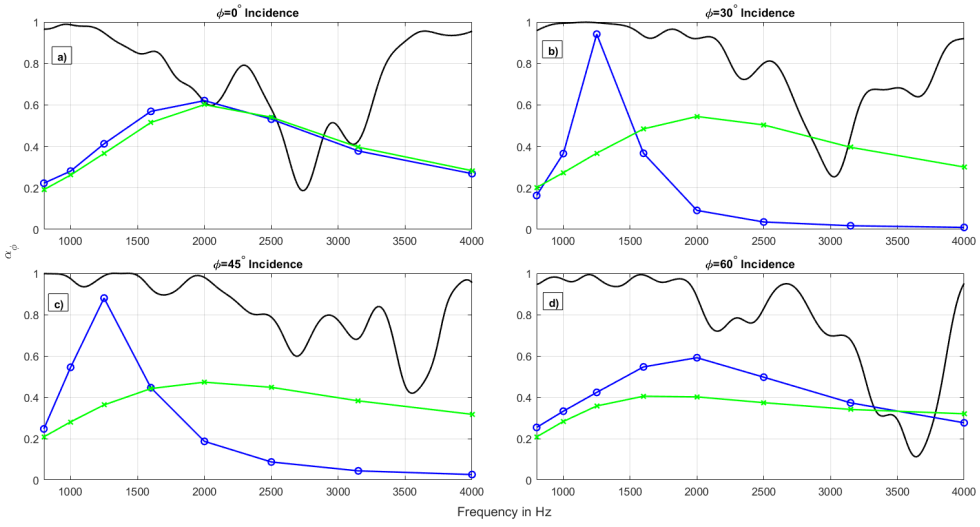

Figure 7: Absorption coefficient of fabricated absorber,a)$\phi = 0°$,b)$\phi = 30°$,c)$\phi = 45°$,d)$\phi = 0°$,(-)Temporal subtraction method,(-o) Finite absorber, (-x) Infinite absorber

The temporal subtraction method as per [1] is based on the part of the energy reflected in non-specular way and not captured by the microphone as being absorber. Knowing this and the fact that the fabricated absorber, due to its finite size would not be able to accommodate wavelengths for frequencies below 857 Hz and 1.14 kHz(based on length and width of the sample, respectively.), shows an overestimation in the absorption coefficient. Furthermore, higher frequencies are more susceptible to non-specular reflection than lower frequencies owing to their shorter wavelength.
For normal incidence (7,a), the infinite absorber and finite absorber curves are near identical while for the temporal subtraction method, the curve deviates in the lower and upper frequency range. As the incident angle increases (7,b-d),the absorption coefficient for the infinite absorber decreases and the finite absorber still shows higher absorption. However, the resonance peak shifts. In the case of temporal subtraction method, though the general curve seems to follow the finite absorber curve, the deviation in the values for absorption coefficient is large due to the over estimation by non-specular reflection.

5
Conclusion

The aim of the master thesis was to study and design sound absorbers suited for the application in corridors while making use of the existing furnitures to mount them and investigate the behaviour of sound incident angle in non-diffuse sound field conditions. This was accomplished in the form theoretical validation and measurements.

The resulting design of the absorber consisting of micro-perforated panel, air-gap and porous absorber, which borrowed the advantages of each of them while compensating for their individual disadvantages. The performance of the absorber in diffuse sound field conditions, both in theoretical and experimental values were well within the expected behaviour, owing to its finite size and phenomenon such as edge effect. From the investigation of the angle-dependent incidence, the results were similar in terms of the shape for the respective angles but the values of absorption coefficient differed at the high frequency region. The measurement had its drawbacks since it was based on the non-specular reflection captured as absorbed, leading to over estimation of the absorption coefficient and lack of compensation for the finite size of the absorber was seen in the method procedure. Even though such drawbacks and uncertainty was encountered, the practical working of the absorber can be seen as a positive.

The thesis provides a tiny step into the pragmatic solutions for absorbers and sound field in corridors. With the investigation of the effective parameters such as perforation constant, flow resistivity, thickness of porous material and air gap, towards the design of the absorber and low cost of fabrication, multiple absorber with different effective parameters can be considered to be housed on such furnitures. Thus catering to different frequencies of interest and overcoming the hurdles of a single finite size absorber.

Bibliography

[1] Acoustics – measurement of sound absorption properties of road surfaces in situ – part 1: Extended surface method, 2022.

[2] Building acoustics - sound requirements for spaces in buildings - healthcare premises, rooms for education, preschools and leisure-time centres, rooms for office work, hotels, and restaurants, 2023. SS 25268:2023.

[3] Eric Brandao, Arcanjo Lenzi, and Stephan Paul. A review of the in situ impedance and sound absorption measurement techniques. *Acta Acustica united with Acustica*, 101, 06 2015.

[4] Eddy Bøgh Brixen. Facts about speech intelligibility. *https://www.dpamicrophones.com/mic-university/background-knowledge/facts-about-speech-intelligibility*, -.

[5] M.E. Delany and E.N. Bazley. Acoustical properties of fibrous absorbent materials. *Applied Acoustics*, 3(2):105–116, 1970.

[6] International Organization for Standardization. Acoustics – rating of sound insulation in buildings and of building elements – part 1: Airborne sound insulation, 2020.

[7] International Organization for Standardization (ISO). Acoustics – measurement of sound absorption in a reverberation room, 2003.

[8] Noé Jiménez, Jean-Philippe Groby, and Vicent Romero-García. *The Transfer Matrix Method in Acoustics*, pages 103–164. Springer International Publishing, Cham, 2021.

[9] Jian Kang. The unsuitability of the classic room acoustical theory in long enclosures. *Architectural Science Review*, 39(2):89–94, 1996.

[10] H Kuttruff. *Acoustics: An Introduction (1st ed.)*. CRC Press, 2006.

[11] Bilgin A. S Laghigna, A. Survey: Sound in schools and its impact on learning and teachers' wellbeing. european schoolnet. *European Schoolnet (EUN Partnership AIBSL)*, 2023.

[12] D. Y. Maa. Microperforated-panel wideband absorbers. *Noise Control Engineering Journal*, 29:77–84, 1987.

[13] D. Y. Maa. Potential of microperforated panel absorber. *Journal of the Acoustical Society of America*, 104:2861–2866, 1998.

[14] Rindel J. Lord P. Maekawa, Z. *Environmental and Architectural Acoustics (2nd ed.)*. CRC Press, 2010.

[15] E.T. Paris. L. on the coefficient of sound-absorption measured by the reverberation method. *The London, Edinburgh, and Dublin Philosophical Magazine and Journal of Science*, 5(29):489–497, 1928.

[16] Kerstin Persson Waye, Sofie Fredriksson, Laith Hussain-Alkhateeb, Johanna Gustafsson, and Irene van Kamp. Preschool teachers' perspective on how high noise levels at preschool affect children's behavior. *PLOS ONE*, 14(3):1–13, 03 2019.

[17] Xiaojun Qiu. *Principles of Sound Absorbers*, pages 43–72. Springer Singapore, Singapore, 2016.

[18] J.H. Rindel. Modelling the angle-dependent pressure reflection factor. *Applied Acoustics*, 38(2):223–234, 1993.

[19] Std Samhäll. Building acoustics – sound requirements for spaces in buildings–healthcare premises, rooms for education, preschools and leisure-time centres,rooms or office work, hotels, and restaurants. Standard, Swedish Institute for Standards, Stockholm, Sweden, 2023.

[20] Hengling Song. Effect of varying corridor parameters on signal-to-noise ratio in classrooms. *Acoustical Science and Technology*, 44:110–119, 03 2023.

[21] Building Swedish Board of Housing and Planning. Boverket's building regulations, bbr18 - (bfs 2011:26), 2011. Accessed: 2024-08-12.

[22] S.-I. Thomasson. On the absorption coefficient. *Acta Acustica united with Acustica*, 44(4):265–273, 1980.

[23] Tor Erik Vigran. *Building Acoustics*. CRC Press, 2008.

[24] Teruji Yamamoto. On the distribution of sound energy along a corridor. *The Journal of the Acoustical Society of Japan*, 17:286–292, 1961.